Materials Research Express

PAPER • OPEN ACCESS

Remarkable photocatalytic degradation of Remazol Brilliant Blue R dye using bio-photocatalyst 'nano-hydroxyapatite'

To cite this article: Sumayya Begum *et al* 2020 *Mater. Res. Express* **7** 025013

Materials Research Express

OPEN ACCESS

RECEIVED
4 October 2019

REVISED
21 January 2020

ACCEPTED FOR PUBLICATION
23 January 2020

PUBLISHED
4 February 2020

PAPER

Remarkable photocatalytic degradation of Remazol Brilliant Blue R dye using bio-photocatalyst 'nano-hydroxyapatite'

Sumayya Begum[1], **Vijaykiran N Narwade**[1], **Devidas I Halge**[1], **Suhas M Jejurikar**[2], **Jagdish W Dadge**[3], **Subas Muduli**[4], **Megha P Mahabole**[1] and **Kashinath A Bogle**[1]

[1] School of Physical Sciences, Swami Ramanand Teerth Marathwada University, Nanded-431606, India
[2] National Center for Nanoscience and Nanotechnology, University of Mumbai, Mumbai-400098, India
[3] Department of Physics, College of Engineering, Pune-411005, India
[4] Department of Physics, Indian Institute of Science Education and Research, Pune-411008, India

E-mail: kashinath.bogle@gmail.com

Keywords: photocatalysis, hydroxyapatite, remazol brilliant blue R dye, degradation

Abstract

Nanostructured bio-photocatalyst hydroxyapatite (HAp) was synthesized by a simple and productive wet chemical precipitation method to explore the photocatalytic performance of the material for degradation of Remazol Brilliant Blue R (RBBR) dye. Wet chemically synthesized nano-HAp was characterized through x-ray diffraction, Transmission electron microscope, scanning electron microscope, N_2-adsorption–desorption, thermo gravimetric analyzer, Fourier transform infrared and UV–vis absorption techniques. Photocatalytic degradation of RBBR under ultraviolet irradiation was examined and ~80% degradation was achieved in 120 min by using nano-HAp. The photocatalytic degradation followed Parabolic Diffusion kinetics. Fast degradation kinetics and removal of RBBR dye was achieved by nano-HAp due to modification of surface entities leading to suppression of photo-generated electron-hole recombination. This makes nano-HAp a remarkable bio-photocatalyst material for removing dyes from water.

1. Introduction

Rapid industrialization across the world raises an environmental problem like water pollution. To overcome with this, photocatalysis using various metal oxide semiconducting materials [1, 2] has received a great attention across researchers [3–5]. During photocatalytic degradation, the photocatalyst is excited by ultraviolet (UV)/ visible photons to generate electron-hole pairs. These photo-induced charges separate and migrate to the active reaction sites and at last on the surface of the photo-catalyst the pollutant is reduced and degraded. Pollutants in water are generally in the form of dangerous organic or inorganic materials; including heavy metals, chemicals, dyes, etc [6–8]. Existences of such pollutants are serious threat to public health and leading to the destruction of ecosystem [9].

Photocatalytic dye degradation does not require any extra effort for treating waste water. This technology requires material with high stability, non-toxicity, photo-generating radical characteristic and wide band gap [10–16]. Binary metal oxides (such as ZnO, TiO_2, ZrO_2, etc) have wide band-gap energy, whichresults in recombination of photo-generated electron-hole pairs leading to low photocatalytic activity [5]. Hydroxyapatite (HAp) is a bio-compatible material found in human bones. HAp is thermal stable, non-toxic with ion exchange capability. Itwasutilized in bulk form (crystallite size in μm) as a photo-catalyst for dye degradation [15, 17, 18] and was found to be low photoactive [5].

One of the best methods to improve the photocatalytic performance of HAp is the selection of synthesis method, which provides nano-HAp crystals. A number of routes, including sol-gel, chemical precipitation, hydrothermal and plasma oxidation methods were developed so far [5, 15]. These methods are costly or inefficiency or high energy consuming,therefore, it is still challenging to prepare nano-HAp.

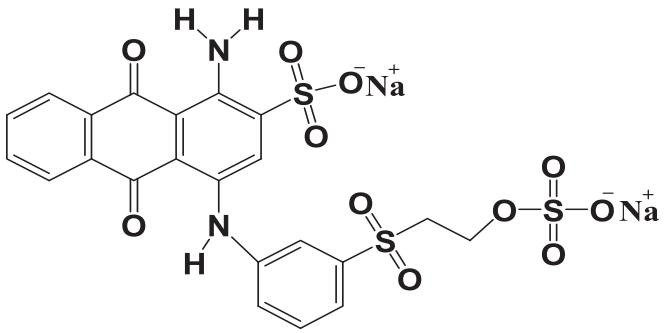

Figure 1. Molecular structure ofRemazol Brilliant Blue R (RBBR) Dye.

In the present work, nano-HAp have been synthesized, characterized and tested as photocatalyst for degradation of RBBR dye under UV light irradiation. HAp is a stable biomaterial used in heterogeneous photocatalytic degradation of pollutants and it also used as a photocatalyst under UV irradiation. The electronic state of the surface PO_4^{3-} group changes to create a vacancy on HAp surface and the electron is transferred to the surrounding oxygen followed by the formation of O_2° radicals. The generated superoxide radical will oxidize the organic molecule and also may react with the water molecule. The induced OH radicals oxidize the pollutant organic molecules adsorbed on to the photo-catalyst. These phenomena on the HAp would be due to photo-induced electronic excitation. The effect of dye concentration on photocatalytic activity of nano-HAp has been studies. A kinetic study was also conducted for finding the photocatalytic degradation model.

2. Experimental

Nano-HAp was synthesized by a wet chemical precipitation method. In this method, di-ammonium hydrogen phosphate ($(NH_4)_2HPO_4$), calcium nitrate tetra hydrate ($Ca(NO_3)_2.4H_2O$), ammonia solution (NH_4OH) purchased from Sigma Aldrich Corporation are used. The synthesis processstarts withdrop wise addition of 0.6M di-ammonium hydrogen phosphate solution in 1M calcium nitrate tetrahydrate solution under vigorous stirring at 80 °C for 3 h [19, 20] by keeping pH constant at 10. Subsequently, the obtained milky white viscous gel was aged for 24 h and later washed with distilled water to remove impurities. Herein the obtained paste was further dried at 100 °C.

The RBBR ($C_{22}H_{16}N_2Na_2O_{11}S_3$) is a synthetic dye (procured from Fluka® Analytical) and is difficult to degrade, therefore, discharged in water streams by the industries. The RBBR is a water soluble anionic anthraquinonereactive toxic dye [18] and itsmolecular structure is shown in figure 1. The photo-catalytic activity of the nano-HAp was measured by testing the degradation of RBBR dye under UV light irradiation. Photo-catalysis experiment was carried out by preparing a stock solution of RBBR dye by mixing 0.1 g of RBBR dye in 1 liter water. RBBR dye solution of three different concentrations (10, 30 and 60 mg l^{-1}) was prepared by diluting the concentrated solution and labeled as sol-A, sol-B and sol-C, respectively. The volume for each solution is kept to be 50 ml and 25 mg of nano-HAp was added to each solution. This mixture was then kept in the photochemical UV reactor for irradiation. 5 ml of suspension was withdrawn periodically (5, 10, 20, 45, 60, 120, 180 and 240 min) and filtered to remove HAp. The concentration of the residual RBBR dye was analyzed by checking the absorbanceat 595 nm with a UV–vis spectrophotometer [21]. The ratio of the nano-HAp catalyst to RBBR dye were catalytically determined to check the effect of contact time of nano-HAp with RBBR dye solution in presence of UV light and hence to check its kinetics., The percentage degradation was estimated by taking ratio of C/C_0. Where C_0 is the initial dye concentration in the solution (mg/l) and C is the final dye concentration in the solution (mg/l) at different time periods.

$$\text{Percentage Degradation} = \left(1 - \frac{C}{C_0}\right) * 100 \tag{1}$$

The structural, thermal, morphological and optical analysis of the nano-HAp was carried out using x-ray diffraction (XRD), transmission electron microscope (TEM), scanning electron microscopy (SEM), thermo-gravimetric analysis (TGA), Brunauer–Emmett–Teller (BET)analysis, Fourier transform infrared spectroscopy (FTIR) and UV–vis absorption spectroscopy, respectively.

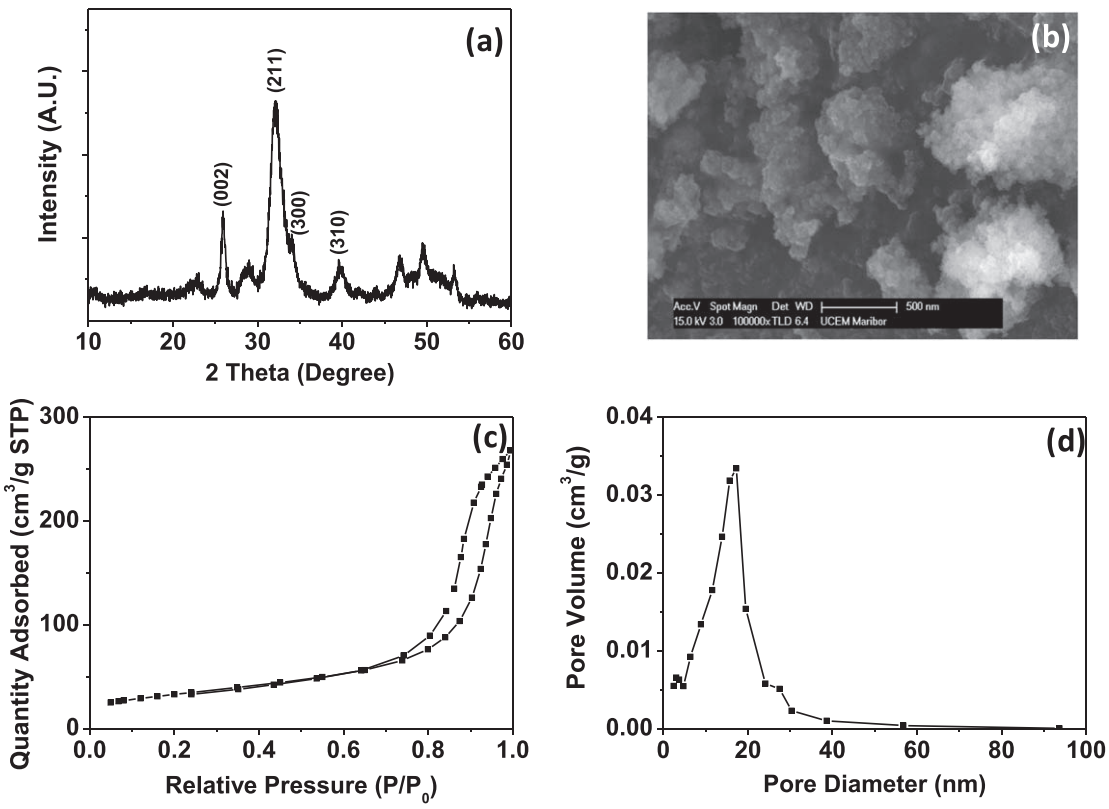

Figure 2. (a) XRD pattern, (b) SEM micrograph, (c) and (d) BET analysis for calculating specific area and pore diameter of wet chemically synthesized nano-HAp.

3. Results and discussion

Figure 2(a) show the XRD pattern of synthesized nano-HAp. The diffraction peaks appeared at 25.8°, 31.8°, 32.9°, and 34.1° corresponds to (002), (211), (300) and (310) crystalline planes of HAp(JCPDS #009-0432) [20]. The broad nature of XRD peaks indicates nano-HAp with average crystallite size ~9 nm estimated using Debye–Scherrer's formula. The intensities of diffraction peaks suggest that higher temperature calcination allows complete crystallization of HAp. SEM image in figure 2(b) show large size agglomerates of nano-HAp crystallites.

The BET analysis of nano-HAp is shown in figures 2(c) and (d). The N_2 adsorption–desorption isotherm curves for nano-HAp (figure 2(c)) reveals the type IV isotherm with H_4 hysteresis loop typically obtain for mesoporous material. The BJH mesoporous fitting model/pore distribution calculation scheme of nano-HAp, figure 2(d), indicates that the average pore diameter is ~17.5 nm, which is in the mesoporous range (between 2–50 nm). The estimated specific surface area of nano-HAp is 118.02 $m^2\ g^{-1}$.

Figure 3(a) show thermal stability of the nano-HAp. A negligible weight loss of ~5% reveals good thermal stability of wet chemically synthesized nano-HAp [21]. The FTIR spectrum of HAp (in figure 3(b)) match with the reported spectra in literature [19, 22]. The strong and sharp peaks at 1031 and 567 cm^{-1} corresponding to the stretching and bending modes of the phosphate groups (PO_4^{3-}) in HAp, respectively [21]. The P–O bending vibration mode of HAp is observed around 610 cm^{-1}. The diffuse-reflectance UV–Vis spectrum of nano-HAp powder is shown in figure 3(c). The band gap estimated from the spectrum is ~3.99 eV. The band gap of nano-HAp material is found to be nearly in the same range of semiconducting material [23, 24]. Hence, it is concluded that the nano-HAp material can perform the photocatalytic reactions under UV irradiation.

The size and shape of nano-HAp was investigated using TEM and shown in the figure 4. TEM images reveal the agglomerates of elongated shape of nano-HAp particles with length of ~50 nm and width of ~10 nm. Fine holes observed across the nano-HAp particles in the magnified TEM image indicate porous nature of the nano-HAp particles. The SAED pattern also indicates the crystalline nature of nano-HAp and is found to be consistent with the XRD results shown in figure 2(a).

The detailed study of adsorption of RBBR dye on nano-HAp in dark conditions was also performed to validate physisorption of RBBR dye on nano-HAp surface (figures 5(a) and (b)). For this adsorption experiment, the dye solution (sol-A) containing 25 mg of nano-HAp was kept in dark environment. The UV–vis absorption

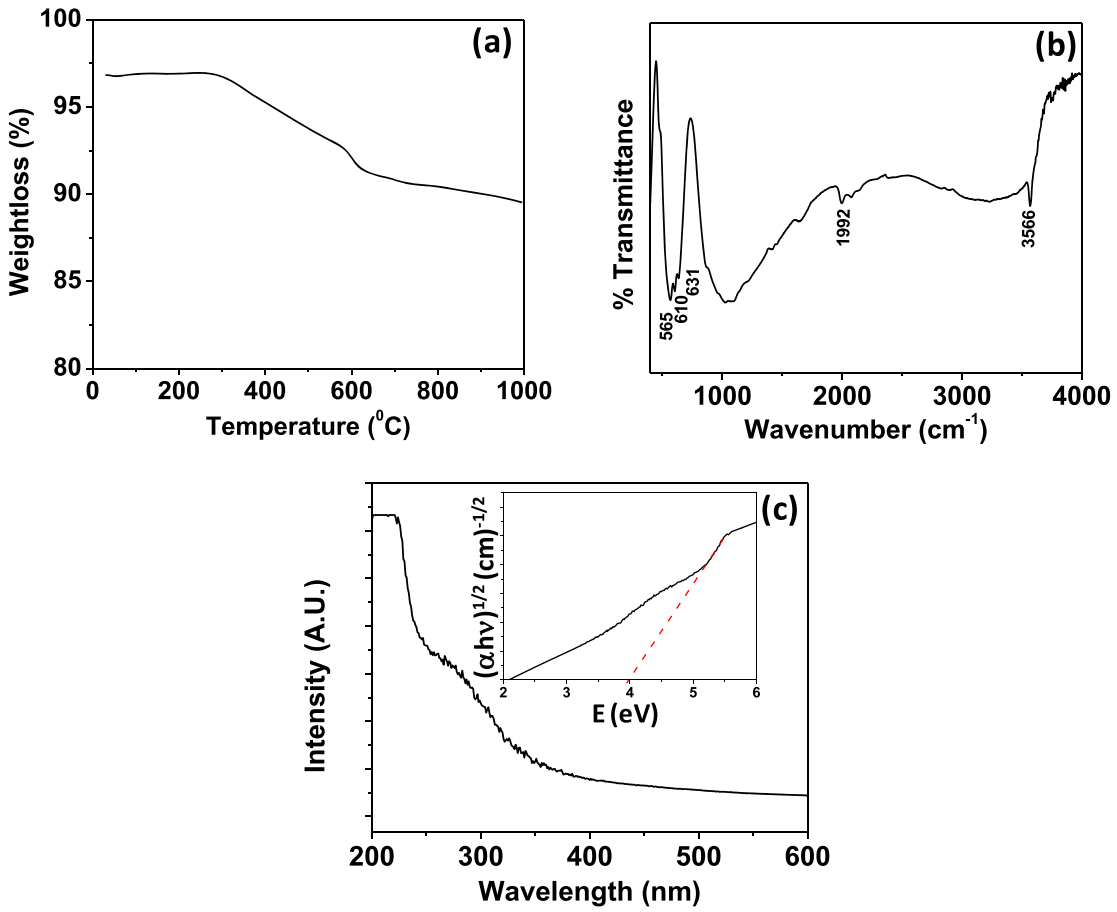

Figure 3. (a) Thermogram, (b) FTIR spectra, (c) UV–vis absorption spectra for wet chemically syntehesized nano-HAp powder. Inset in (c) show Tauc fitting of absorption spectra.

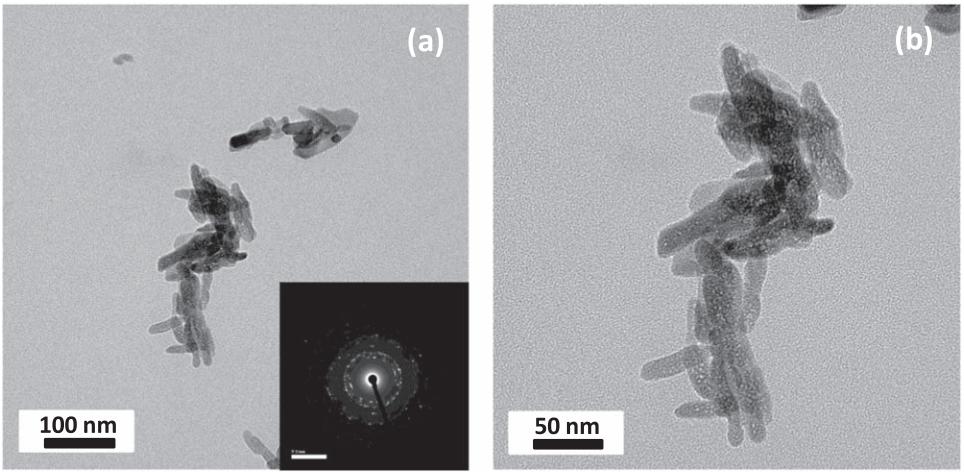

Figure 4. (a) and (b) TEM images of nano-HAp particles (inset show SAED pattern).

graph of the Sol-A measured at different interval depicts almost ~50% dye adsorption in first 5 min, which remains constant up to 180 min. After that, photocatalytic activity of nano-HAp was evaluated by monitoring the degradationof RBBR concentration (C/C_0) as a function of irradiation time and the obtained results are shown in figure 6. For dye solution (sol-A without nano-HAp), figure 6(a),the degradation is ~25% in 120 min UV irradiation, whereas,after 25 mg nano-HAp addition it enhances significantly to ~70% in first 5 min and later to ~80% in 120 min of UV irradiation figure 6(b). This addition indicates that presence of nano-HAp in

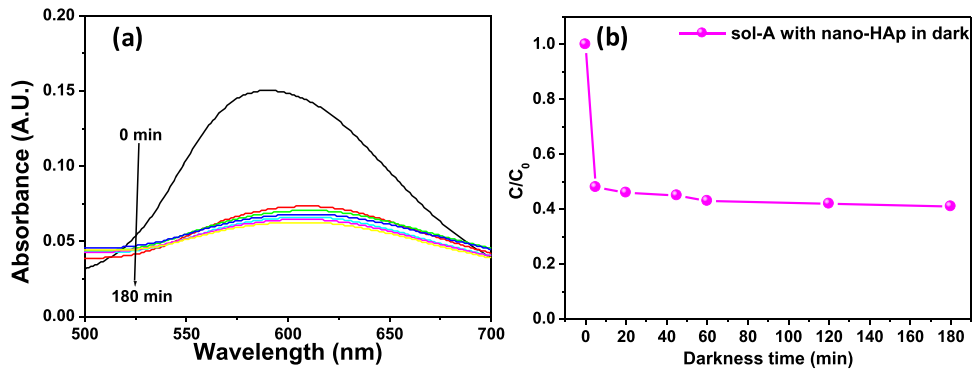

Figure 5. (a) UV–vis absorption spectra and (b) Adsorption efficiency graph for the 10 mg l^{-1} dye degradation in presence of 25 mg HAp without UV–vis light irradiation i.e. in dark as well as without stirring.

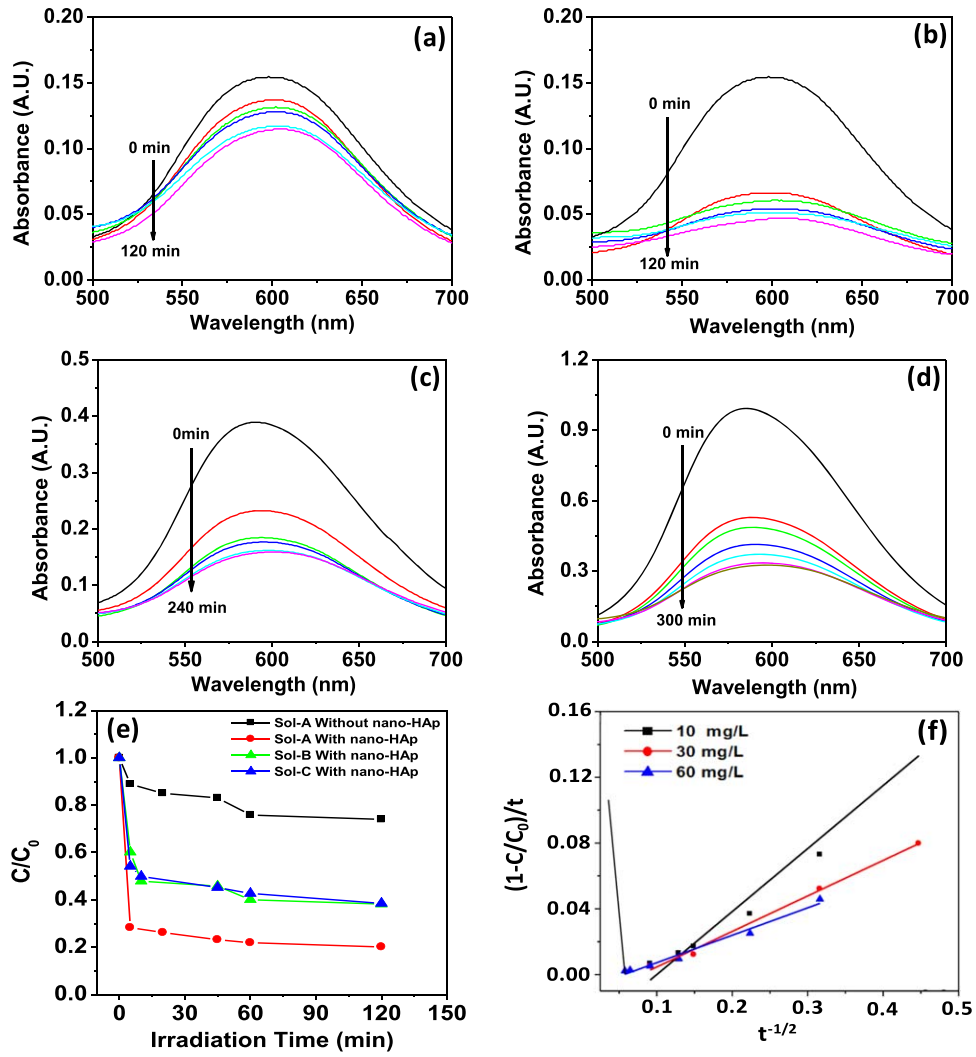

Figure 6. Photocatalytic degradation of RBBR dye with irradiation time for various dye concentrations (10, 30 and 60 mg l^{-1}) in absence of nano-HAp and (b) Parabolic Diffusion model kinetics for various dye concentrations.

sol-A is beneficial to enhance photocatalytic activity. Similar results were obtained for nano-HAp added sol-B and sol-C, whereas, the degradation is ~60% in 120 min, but could not achieve 80% even in 300 min UV irradiation (figures 6(c) and (d)). It can be noted that the photocatalytic degradation rate follows the Parabolic Diffusion model kinetics (figure 6(f)). This important result confirms that nano sized HAp crystals acts as

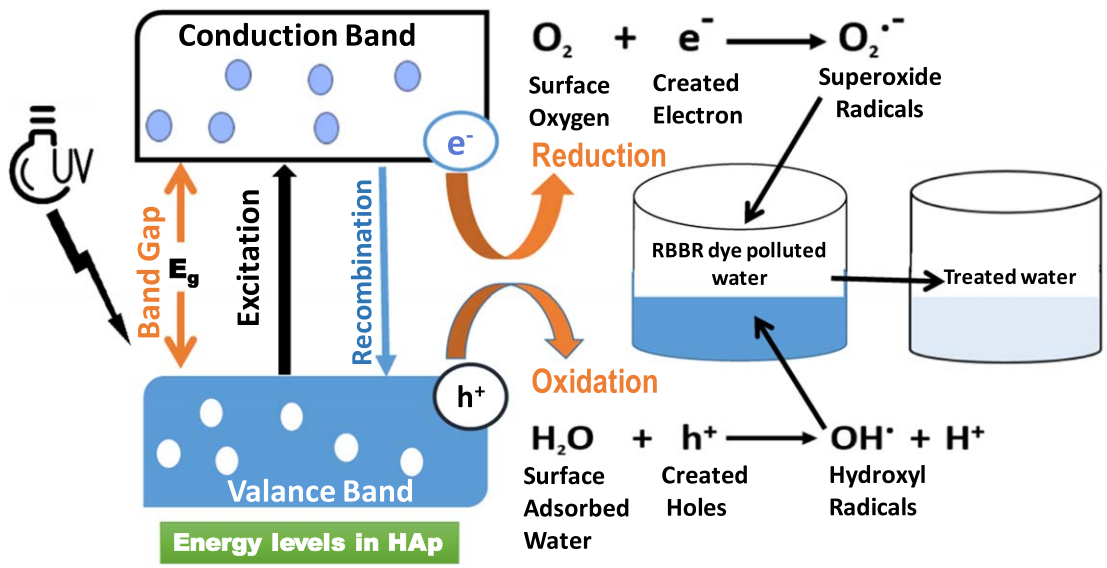

Figure 7. Schematic representation of photocatalytic process occurred during degradation of RBBR dye using radicals generated by photoactive nano-HAp.

photo-catalysts and induces photocatalytic processes (generation of OH. and O_2^- radicals on the surface of nano-HAp) under UV irradiation [25–27], which are responsible for enhanced dye degradation. However, at higher dye concentration, the percentage of radicals with respect to dye concentration remains low and may be responsible for lower degradation of dye.

The interaction of UV light with RBBR dye solutions containing nano-HAp catalyst follow two processes; degradation and adsorption, as discussed earlier. First, UV photon interacts with nano-HAp and imparts its energy to electron, this excited electron jumpsto the conduction band and leaving a hole in the valance band. At the same time, the RBBR also get excited and the excited dye transfers an electron into the conduction band of the nano-HAp or the dye directly reacts with the valance band's holes, as shown in figure 7. The second possibility of RBBR dye degradation in presence of nano-HAp is summarized as [28–33],

i. As HAp is amphoteric in nature (i.e. existence of H^+ and OH^- ions), its surface can capture outer water molecule. At the same time,electron from conduction band of HAp get capture by the surface oxygen (O_2) giving superoxide anion radicals ($O^\circ{}_2$), referred as oxygen ionosorption [25, 34].

ii. On the other hand, valence band holes get neutralize with OH^- ions and then it will give hydroxyl radical (OH°). Then these radicals undergo redox reactions.

iii. The radicals and/or ionic species formed can react further, to form more species, which are referred to as Reactive Oxygen Species (ROS). The generated superoxide anion radicals ($O^\circ{}_2$) again react with valence band holes which produce protonated super oxide radical ($HO^\circ{}_2$). This protonated super oxide radical ($HO^\circ{}_2$) reacts with super oxide radical ($O^\circ{}_2$) and holes. ROS can then react with molecules of organic contaminants (in our case it is RBBR dye molecule) and eventually lead to degradation of these molecules.

iv. Subsequently, above mentioned interactions give hydrogen peroxide (H_2O_2) and oxygen (O_2) molecule which can further react and enhance the OH radicals and also inhibit the electron/hole (e^-/h^+) pair recombination.

These two steps generates hydroxyl radicals which interact with reactive site of RBBR for degradation. On the other hand, UV radiation directly interact with RBBR and produced (OH) group containing by products and these by product will interact with reactive sites of HAp.

The stability and reusability of a catalyst are essential for its practical application. For nano-HAp catalyst, the recycling tests were carried out under optimal conditions in 3 continuous cycles. For this, used nano-HAp powder was cleaned ultrasonically in hot water to remove the dye on it. The results indicate that the catalytic potential of HAp towards RBBR was well maintained with a slight reduction of degradation efficiency from 80% to 70% after 3 continuous cycles.

4. Conclusion

In summary, nano sized bio-photocatalyst 'HAp' has been synthesized via a simple and low cost wet chemical method with an average crystallite size of ~9 nm. A remarkable photocatalytic degradation of RBBR Dye using bio-photocatalyst 'Nano-hydroxyapatite' was observed under UV light irradiation with ~80% degradation in 120 min, which is almost 3 times higher than the experiment performed without nano-HAp and many times higher than that of bulk HAp. According to its structure/size and photocatalytic activity, nano-HAp show an effective photocatalytic property for removing dye from water and can be used for developing high quality photocatalytic filters in dye industries.

Acknowledgments

Authors would like to acknowledge Prof Pandit B Vidyasagar, Former Vice-Chancellor and Prof Udhav Bhosale, Vice-Chancellor SRTMU Nanded for constant encouragement.

ORCID iDs

Vijaykiran N Narwade https://orcid.org/0000-0001-7186-6571
Suhas M Jejurikar https://orcid.org/0000-0002-5315-7621
Kashinath A Bogle https://orcid.org/0000-0001-9472-3696

References

[1] Khan M M, Adilamd S F and Al-Mayouf A 2015 *Journal of Saudi Chemical Society* **19** 462
[2] Zaleska-Medynska A 2018 *Metal Oxide-Based Photocatalysis* (Netherland: Elsevier Publishing)
[3] Ishchenko O M, Rogé V, Lamblin G and Lenoble D 2016 *TiO_2- and ZnO-Based Materials for Photocatalysis:Material Properties, Device Architecture and EmergingConcepts* (IntechOpen Publishing) pp 3–30 ch 1
[4] Sampa C and Binay K D 2004 *JournalofHazardous Materials B* **112** 269
[5] Han H-re, Qian X, Yuan Y, Zhou M and Chen Y-L 2016 *Water Air Soil Pollut.* **227** 461
[6] Uslu H, Yankov D, Isewar K L, Azizian S, Ullah N and Ahmad W 2015 *Journal of Chemistry* **2015** 3 698259
[7] Järup L 2003 *Br. Med. Bull.* **68** 167
[8] IARC 2006 Working group on the evaluation of carcinogenic risks to humans, inorganic and organic lead compounds *IARC Monographs on the Evaluation of Carcinogenic Risks to Humans* **87** 1
[9] Schwarzenbach R P, Egli T, Hofstetter T B, Von Gunten U and Wehrli B 2010 *Annual Review of Environment and Resources* **35** 109
[10] Narwade V N, Khairnar R S and Kokol V 2018 *J. Polym. Environ.* **26** 2130
[11] Etacheri V, Seery M K, Hinder S J and Pillai S C 2010 *Chem. Mater.* **22** 3843
[12] Etacheri V, Roshan R and Kumar V 2012 *ACS Applied Materials &Interfaces* **4** 2717
[13] Liu Y, Yu L, Hu Y, Guo C, Zhang F and Lou X W D 2012 *Nanoscale* **4** 183
[14] Chu D, Mo J, Peng Q, Zhang Y, Wei Y, Zhuang Z and Li Y 2011 *Chem. Cat. Chem.* **3** 371
[15] Nishikawa H and Omamiuda K 2002 *J. Mol. Catal. A: Chem.* **179** 193
[16] Naraginti S, Stephen F B, Radhakrishnan A and Sivakumar A 2015 *SpectrochimicaActa Part A: Molecular and Biomolecular Spectroscopy* **135** 814
[17] Piccirilloand C and Castro P M L 2017 *J. Environ. Manage.* **193** 79
[18] Novotný C, Dias N, Kapanen A, Malachová K, Vándrovcová M, Itävaara M and Lima N 2006 *Chemosphere* **63** 1436
[19] Mene R U, Mahabole M P and Khairnar R S 2011 *Radiat. Phys. Chem.* **80** 682
[20] Narwade V N and Khairnar R S 2017 *Bull. Pol. Acad. Sci. Tech. Sci.* **65** 131
[21] El-Ashtoukhy E S, Mobarak A A and Fouad Y O 2016 *Int. J. Electrochem. Sci.* **11** 1883
[22] Tank K P, Sharma P, Kanchan D K and Joshi M J 2011 *Cryst. Res. Technol.* **46** 1309
[23] Rulis P, Ouyang L and Ching W Y 2004 *Physical Review B* **70** 155104
[24] Wei X J, Li Y H, Qin Z B and Cui G H 2019 Two zinc (II) coordination polymers for selective luminescence sensing of iron (III) ions and photocatalytic degradation of methylene blue *J. Mol. Struct.* **1175** 253–60
[25] Sheng G, Qiao L and Mou Y 2011 *J. Environ. Eng.* **137** 611
[26] Li J X, Liu D, Qin Z B and Dong G Y 2019 Sonochemical synthesis of two nano-sized nickel (II) coordination polymers derived from flexible bis (benzimidazole) and isophthalic acid ligands *Polyhedron* **160** 92–100
[27] Wei X J, Liu D, Li Y H and Cui G H 2019 New 2D and 3D Cd (II) coordination polymers from aromatic dicarboxylate and 1, 3-bis (5, 6-dimethylbenzimidazol-1-yl)-2-propanol ligands: syntheses, structures, photocatalytic, and luminescence sensing properties *J. Solid State Chem.* **272** 138–47
[28] Xie X, Li X, Luo H, Lu H, Chen F and Li W 2016 *The Journal of Physical Chemistry B* **120** 4131
[29] Fanchiang J M and Tseng D H 2009 *Chemosphere* **77** 214
[30] Mourid E, Lakraimi M, El Khattabi E, Benaziz L and Berraho M 2017 *J. Mater. Environ. Sci,* **8** 921
[31] Fanchiang J M and Tseng D H 2009 *Environ. Technol.* **30** 161
[32] Eichlerová I, Homolka L, Benada O, Kofroňová O, Hubálek T and Nerud F 2007 *Chemosphere* **69** 795
[33] Yonten V, Tanyol M, Yildirim N, Yildirim N C and Ince M 2016 *Desalin. Water Treat.* **57** 15592
[34] Houas A, Lachheb H, Ksibi M, Elaloui E, Guillard C and Herrmann J M 2001 *Appl. Catalysis B* **31** 145